Examining the Effectiveness of Ballast Water Treatment Processes: Insights into Hydrocarbon Oxidation Product Formation and Environmental Implications

Maxwell L. Harsha*[a], David C. Podgorski[a,b,c,f]

[a]Department of Chemistry, [b]Chemical Analysis & Mass Spectrometry Facility, [c]Pontchartrain Institute for Environmental Sciences, Shea Penland Coastal Education and Research Facility, University of New Orleans, 2000 Lakeshore Drive New Orleans, Louisiana, USA

*Corresponding Author: mlharsha@uno.edu

Abstract:

This study investigates the treatment processes employed at a ballast water treatment facility in Valdez, Alaska, to remove hydrocarbons from unsegregated ballast water. Specifically, the aim is to quantify and characterize hydrocarbons of emerging concern, known as hydrocarbon oxidation products (HOPs), and heavy metals (HMs) throughout the treatment process. Specialized analytical techniques, such as non-volatile dissolved organic carbon analysis, fluorescence excitation-emission matrix spectroscopy, and inductively coupled plasma triple quadrupole mass spectrometry were employed for quantification and characterization. Results demonstrate that the treatment process effectively removes benzene, toluene, ethylbenzene, and xylene (BTEX) compounds, while HOPs remain. Optical analyses provide insights into the composition and transformation of HOPs, showing a shift towards more oxygenated and complex compounds during the treatment process. Additionally, the study examines the concentrations of various HMs and identifies their trends throughout the treatment process. The findings highlight the need for comprehensive monitoring and regulation of ballast water treatment processes, considering the presence of HOPs and HMs. The results provide valuable insights for environmental monitoring and risk assessment in ballast water treatment, emphasizing the significance of understanding and mitigating the impacts of petroleum derived contaminants on aquatic ecosystems.

Keywords:

Fluorescence, PARAFAC, oxyhydrocarbons, DOM, oil spill, biodegradation, stormwater, wastewater, ICP-QQQ, heavy metals

Table of Contents

Acronym List

ADEC	Alaska Department of Environmental Conservation
APDES	Alaska Pollutant Discharge Elimination System
BT	Biological Treatment
BTEX	Benzene, Toluene, Ethylbenzene, and Xylene
BWTF	Ballast Water Treatment Facility
C[1,2,3,…]	Component [1,2,3,..]
CO_2	Carbon Dioxide
DAF	Dissolved Air Flotation
EEMs	Excitation-Emission Matrix Spectroscopy
EX/EM	Excitation and Emission Maxima
G	Grams
GS	Gravity Separation
HDPE	High Density Polyethylene
HIX	Humification Index
HMs	Heavy Metals
HOPs	Hydrocarbon Oxidation Products
ICP-QQQ	Inductively Coupled Plasma Triple Quadrupole Mass Spectrometry
KG	Kilograms
LOD	Limit of Detection
LOQ	Limit of Quantification
MG/L	Milligrams per Liter
ML	Milliliters
MM	Millimeters
NaOH	Sodium Hydroxide
NM	Nanometers
NVDOC	Non-Volatile Dissolved Organic Carbon Analysis
PAHs	Polycyclic Aromatic Hydrocarbons
PARAFAC	Parallel Factor
PCA	Principal Component Analysis
pH	Potential of Hydrogen
S	Seconds
$SUVA_{254}$	Specific UV absorbance at 254 nm
TAH	Total Aromatic Hydrocarbons
TAqH	Total Aqueous Hydrocarbons
THM	Total Concentration of Heavy Metals
TP	Tank Prior
UCM	Unresolved Complex Mixture
µm	Micrometer

Executive Summary

Ships rely on ballast water to maintain stability when traveling without cargo. However, this water can contain pollutants, including hydrocarbons derived from oil, when stored in cargo tanks. When this unsegregated ballast water is discharged, these pollutants can be released into environments where they pose risk to the health of aquatic ecosystems. Ballast water treatment facilities (BWTFs) are designed to eliminate these oily contaminants before water is returned to the environment.

Current regulations on the effectiveness of the removal of oily contaminants are based on the concentration of four compounds: benzene, toluene, ethylbenzene, and xylene (BTEX). However, these four compounds only account for a tiny fraction of crude oil. Most compounds in petroleum are not accounted for by these measurements. Specifically, hydrocarbon oxidation products (HOPs), which can be more toxic than their parent petroleum compounds, are considered to be emerging contaminants because they are not regulated by government agencies. In addition to enhanced toxicity, HOPs are water-soluble, so they can be rapidly transported vast distances away from their source of origin in aquatic ecosystems. There is limited knowledge about the effectiveness of BWTFs in removing HOPs and potentially toxic heavy metals.

The goal of this research is to determine the removal efficiency of HOPs and heavy metals at the BWTF in Valdez, Alaska, prior to their release into Port Valdez. Over the course of one year, 12 sample sets were opportunistically collected at the Valdez Marine Terminal's BWTF when incoming tankers unloaded unsegregated ballast water (stored in the same tanks as crude oil). Samples were collected after the oil/water separator (90's Tank), dissolved air flotation/air stripper, and biological treatment tank (BTT) prior to discharge into Port Valdez. Most samples were collected in the fall or winter months. Alyeska provided data on BTEX concentrations for each sampling event. HOPs are not detectable by standard methods of analysis that are used to measure hydrocarbons. Therefore, we had to use specialized analytical techniques to measure the chemical composition and concentrations of HOPs at each stage of the treatment process.

The results indicate that the treatment process efficiently removes BTEX as it is designed to do. However, the process does not significantly reduce the concentration of HOPs from the beginning of the process until they are discharged into Port Valdez. Instead, HOPs undergo transformation into more chemically complex and potentially toxic compounds during the treatment process. In addition, the BWTF successfully decreases the concentration of heavy metals released into Port Valdez to meet water quality standards. Although the levels of

these contaminants were not alarmingly high, they can still pose risk to aquatic ecosystems via bioaccumulation.

Recommendations for the future include testing the toxicity of the effluent released into Port Valdez, online monitoring of HOPs with sensors (like BTEX), treating the effluent with light (destroy compounds), and properly maintain microbial populations in BTT (destroy compounds). Moreover, measurements should be made of metals and HOPs in sediments and shellfish (like previous studies focused on hydrocarbons by Dr. Merv Fingas) near the exit of the effluent.

1. Introduction:

Approximately 10 billion tons of ballast water are transported worldwide annually to stabilize cargo ships during their empty voyages between ports (Lamoureux and Organization 1967). However, the offloading of ballast water raises concerns regarding the transfer of harmful biological agents, such as invasive species and pathogens, as well as the release of chemical contaminants (Kurniawan et al. 2022). While the threat of chemical pollution from ballast water offloading decreased with the use of modern double-hulled ships with ballast water tanks segregated from cargo tanks, the North American petroleum industry still faces risks. During winter months, ships may require additional ballast water, which requires storage in unsegregated tanks (Love 2018). Unsegregated ballast water from oil tankers can mix with residual petroleum products, posing a risk of releasing harmful hydrocarbons and oxygen-containing analogues into marine ecosystems. Thus, treatment is necessary before discharging such water into the environment (Verna and Harris 2016).

This study focuses on the ballast water treatment facility (BWTF) at the Valdez Marine Terminal in Prince William Sound, Alaska, operated by the Alyeska Pipeline Service Company. Three treatment processes are employed to remove hydrocarbons from unsegregated ballast water: gravity separation, pressurized air treatment, and biological treatment. These techniques utilize physical (separation and volatilization) and chemical (oxidation) processes to eliminate hydrocarbons before discharging 1.72 million gallons of effluent daily (average) into Port Valdez, an area of significance for aquaculture and conservation (ADEC 2019).

The influent sources at the BWTF are categorized as follows in terms of contribution: stormwater (44%), oiled ballast water (37%), industrial wastewater (14%), and raw water (5%) (ADEC 2019). Stormwater, originating from rain and snowmelt, accounts for the largest influent source and is expected to be uncontaminated, diluting contaminants from other sources (ADEC 2019). Ballast water is the second largest influent source, primarily responsible for hydrocarbon and metal contamination (ADEC 2019). The BWTF discharge has been monitored since 1972 by government agencies, including the Environmental Protection

Agency and the Alaska Department of Environmental Conservation (ADEC). ADEC currently oversees the facility through the Wastewater Discharge Authorization Program (Alaska Pollutant Discharge Elimination System (APDES) permit AK0023248), which mandates monitoring of various parameters in the BWTF effluent, such as flow, pH, total suspended solids, zinc, total aromatic hydrocarbons (TAH), total aqueous hydrocarbons (TAqH), total recoverable oil and grease, density, dissolved inorganic phosphorus, ammonia, and toxicity (ADEC 2019). In the most recent permit, ADEC identifies zinc, TAH, and whole effluent toxicity as the three primary parameters of concern, most likely to exceed water quality criteria in the BWTF effluent (ADEC 2019).

Regulating oil contamination levels during the treatment process typically involves measuring the benzene, toluene, ethylbenzene, and xylene (BTEX) family of compounds, also known as TAH (Payne et al. 2005). Although BTEX represents only a small fraction of crude oil, it serves as a standard for regulation (Hollebone 2011). Crude oil consists of a complex mixture of compounds with varying molecular weights (Palacio Lozano et al. 2019; Krajewski, Rodgers, and Marshall 2017; Frysinger et al. 2003). Higher molecular weight compounds form the unresolved complex mixture (UCM) and are challenging to characterize and quantify using traditional chromatography techniques relied upon by current monitoring methods (Farrington and Quinn 2015; McKenna et al. 2013). Furthermore, compounds in crude oil become more polar when oxidized through biotic and abiotic degradation processes (Ward et al. 2018; Ray et al. 2014; D'Auria et al. 2009; Aeppli et al. 2012; Fry and Steenson 2019). The increased polarity, resulting from the addition of oxygen heteroatoms, further complicates the composition and fraction of compounds in the UCM (Boduszynski 1987; Boduszynski and Altgelt 1992; Boduszynski 1988). These polar hydrocarbon oxidation products (HOPs) can readily partition into the aqueous phase, remaining undetected during transportation from their petroleum source (Aeppli et al. 2012; Fry and Steenson 2019; Krajewski, Rodgers, and Marshall 2017; Frysinger et al. 2003; Zito et al. 2019; Ward and Overton 2020; Maki, Sasaki, and Harayama 2001; Freeman and Ward 2022; Brünjes et al. 2022; Ward et al. 2018; Ray et al. 2014; D'Auria et al. 2009; Palacio Lozano et al. 2019).

HOPs are of emerging concern due to their potential risks to human health and the environment, even though they are not currently regulated (Katz et al. 2022; Little et al. 2000). Additionally, the relationship between the chemical composition of HOPs in the UCM and their toxicity remains to be determined. In the context of ballast water treatment (Katz et al. 2022), HOPs may be formed through microbial processes in ballast tanks during transport and within each step of the water treatment process. Although the BWTF process successfully removes BTEX, the impact of the treatment process on the formation of HOPs is unknown. Another emerging concern is the presence of heavy metals (HMs) in ballast water, as their toxicity varies based on elemental composition and concentration. Despite meeting water quality criteria, whole effluent toxicity testing has revealed chronic toxicity to aquatic organisms in some instances (ADEC 2019). Zinc, with its high recorded concentrations in the BWTF effluent, is believed to be the driving parameter for potential toxicity (ADEC 2019). Therefore, this study aims to investigate the concentration and behavior of HOPs and HMs throughout the BWTF process.

To achieve this objective, specialized analytical techniques are employed. Non-volatile dissolved organic carbon analysis (NVDOC) and fluorescence excitation-emission matrix spectroscopy (EEMs) are used to quantify and reveal optical signatures that provide insight into the composition of HOPs, respectively. Inductively coupled plasma triple quadrupole mass spectrometry (ICP-QQQ) is utilized to determine the quantity of a wide range of HMs. This study serves two purposes: first, to understand the formation and transport of HOPs and HMs through the BWTF process, and second, to quantify and characterize the HOPs and HMs released into Port Valdez through the BWTF discharge. The findings of this study hold significant implications for the functionality and monitoring of the BWTF, as they shed light on two poorly understood and reported classes of contaminants.

2. Materials and Methods:

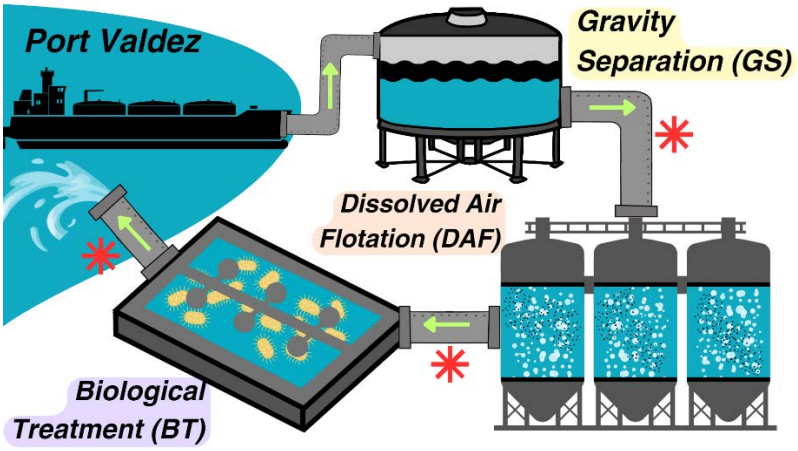

Figure 1. Overview of the BWTF. (*) represents a sampling point.

2.1. BWTF overview and Sample Collection

Figure 1 shows a schematic of the BWTF processing. The process starts with the influent being subjected to gravity separation (GS) in large water storage tanks where settling occurs over an average of four hours. The oil layer is then skimmed and transferred to a recovery tank, while the water layer proceeds to the dissolved air flotation (DAF) process. In the DAF process, air is bubbled through the oiled water to remove volatile organic compounds followed by an air stripping process. Exhaust vapors generated are captured and incinerated using regenerative thermal oxidizers. The treated water then passes to the biological treatment (BT) process, where mixing and aeration occur in large open concrete-lined ponds for an average of 16 hours to promote biodegradation. Finally, the treated water is discharged into Port Valdez.

In Figure 1, the asterisks denote the points at which samples were collected after each treatment process. Opportunistic sampling by the Alyeska Pipeline Service Company took place over one year, resulting in 12 sampling events that corresponded to 12 different ballast water offloading events. To ensure that the same ballast water was captured throughout the treatment process, the sample collection time was staggered at the different process points.

A fourth sampling point was added for the last seven sampling events to collect wastewater from the gravity separation tank prior (TP) to ballast offloading to characterize other sources of influent. Gravity separation tank levels were recorded before and after ballast offloading. Samples were collected using 250 milliliters (mL) amber high density polyethylene (HDPE) bottles and stored at -20°C until analysis. The Alyeska Pipeline Service Company provided BTEX measurements for each sample.

2.2. Non-Volatile Dissolved Organic Carbon (NVDOC) Analysis

HOPs were quantified based on NVDOC concentration. Each sample was filtered through a pre-combusted (550°C > 4 hours) Advantec GF-75 0.3 micrometer (μm) glass fiber filter into a pre-combusted amber glass vial. The pH (potential of hydrogen) of each sample was adjusted with ultrapure hydrochloric acid to pH < 2. Samples were analyzed for NVDOC concentration with a Shimadzu TOC-V system equipped with an autosampler. NVDOC was measured as non-purgeable organic carbon converted to CO_2 (carbon dioxide) and detected by a non-dispersive infrared detector (Stubbins and Dittmar 2012). NVDOC was calibrated with potassium hydrogen phthalate with daily standards run regularly.

2.2. HOPs Optical Characterization

Fluorescence EEMs was utilized to characterize the optical properties of HOPs. The pH of filtered samples was adjusted to pH 8 with NaOH (sodium hydroxide) for absorbance and fluorescence measurements with an Aqualog® fluorometer (Horiba Scientific, Kyoto, Japan) (Yan et al. 2013; Tfaily et al. 2011; Spencer, Bolton, and Baker 2007). Optical measurements were carried out in a 10 millimeters (mm) quartz cuvette, at an excitation range from 240 – 800 nanometers (nm) in 5 nm increments, and an emission range from 240 – 800 nm in 2.34 nm increments with an integration period of 5 seconds (s). Spectra were blank subtracted and corrected for instrument bias and inner filter effects. Fluorescence intensities were normalized to Raman scattering units prior to Parallel Factor (PARAFAC) analysis, a multiway data analysis technique to decompose EEMs into underlying optical signature (Murphy et al. 2013). The drEEM toolbox and MatLab code were utilized to complete PARAFAC of the EEMs

(Murphy et al. 2013). The spectral components of the resulting statistical model were validated by residual and split-half analysis (Harshman and Lundy 1994; Stedmon and Bro 2008). The validated model was uploaded to the OpenFluor database to compare with published models above 95% similarity score (Murphy et al. 2014). Humification index (HIX) values were determined by the peak area under the emission spectra at 435-480 nm divided by the sum peak area at emission spectra 300-345 and 435-480 nm at excitation 254 nm (Ohno 2002). Specific ultraviolet absorbance at 254 nm ($SUVA_{254}$) was calculated by dividing the absorbance at 254 nm (a_{254}) by the NVDOC concentration.

2.3. Heavy Metal Quantification

ICP-QQQ (Agilent Technologies 8900) was utilized to measure the concentration of HMs. A 10 mL aliquot of each sample was filtered through 0.45-µm polypropylene syringe filters (Agilent Technologies) and acidified to a concentration of 2% (v/v) trace-metal grade nitric acid (Fisher Scientific) and 0.5% (v/v) trace-metal grade hydrochloric acid (VWR International). The ICP-QQQ was operated under MS/MS, using helium as the collision gas and ammonia as the reaction gas (Kubota 2022; Proper, Mccurdy, and Takahashi 2020). Quantification of HMs was performed based on calibration curves using environmental calibration standard mix and internal standard mix (Agilent Technologies). The instrument was tuned daily using a solution containing Ce, Co, Li, Mg, Ti, and Y (Agilent Technologies) (1 µg/L). Specific operating parameters and detection limits are outlined in the supplementary information (Tables S1 and S2). Limit of detection (LOD) and quantification (LOQ) calculated from standard deviation of ten blank response replicates and slope of HM calibration curves.

2.4 Statistical Analyses

JMP, Version 17 (SAS Institute Inc.) was used to conduct all statistical analyses. The data underwent Cauchy robust outlier analysis to eliminate any outliers. Pairwise Student's t-tests were employed to calculate p-values at a 95% confidence level. To determine correlation, nonparametric Spearman's rank correlation coefficient (ρ) was used. Principal component analysis was utilized to examine the variation between different processing points.

3. Results and Discussion:

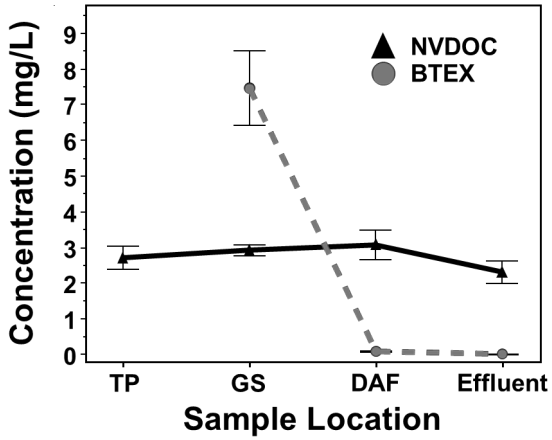

Figure 2. Changes in NVDOC and BTEX concentrations through treatment process.

3.1. Hydrocarbon concentrations through the BWTF process

The measured concentrations of BTEX demonstrate that the BWTF process effectively removes these compounds. Figure 2 shows that BTEX concentrations range from 0.01 ± 0 milligrams per liter (mg/L) in the effluent to 7.47 ± 1.05 mg/L after GS. There is a strong negative correlation (-0.917) between BTEX concentration and treatment processing, indicating the effectiveness of the BWTF process in reducing BTEX levels (Tables S3 and S4). Among the treatment processes, DAF shows the highest efficiency in removing BTEX, as concentrations remain negligible after BT. This result suggests that biodegradation is not a significant factor in removing low concentrations of BTEX from ballast water. These findings align with previous studies investigating the effectiveness of biodegradation at the BWTF (Payne et al. 2005). It is important to note that the measured BTEX levels in the discharge are below the maximum effluent permit limit set by ADEC (0.73 mg/L). The maximum water quality standard for BTEX in Port Valdez is 0.01 mg/L, which is measured at the edge of the BWTF mixing zone (ADEC 2019). Taking into account the subsequent dilution of the effluent in Port Valdez (with a dilution factor of 56:1 in the mixing zone), the measured BTEX values are well below the maximum limit.

In contrast, there is no statistically significant change in the concentration of HOPs as measured by NVDOC among the different treatment processes (Figure 2). The measured NVDOC concentration in the effluent was 2.31 ± 0.31 mg/L (Table S3). It is worth noting that the BWTF does not monitor NVDOC levels directly but instead measures TAqH, which includes BTEX and 16 polycyclic aromatic hydrocarbons (PAHs) to represent the UCM (ADEC 2019). However, this approach is not accurate due to the presence of additional compounds with varying polarity, which makes the UCM unsuitable for gas-chromatography techniques (Farrington and Quinn 2015; McKenna et al. 2013). Currently, there are no specific limits set for TAqH in the BWTF effluent since it is not considered a parameter of concern, although the highest measured concentration in the effluent was 0.04 mg/L (ADEC 2019). The significant difference (~58-fold) between NVDOC and TAqH highlights the complexity of the UCM and the large number of undetected compounds, suggesting that NVDOC is a more effective technique. Currently, there are no regulatory standards for NVDOC concentrations in water quality. However, studies demonstrate the use of NVDOC as an effluent parameter for industrial and municipal treatment processes, providing insight into potentially harmful carbon compounds being released undetected into aquatic ecosystems (Park et al. 2022; Yang et al. 2015).

3.2. Optical signatures reveal compositional changes in HOPs

Optical analyses reveal changes in the composition of HOPs, providing insights into their source, reactivity, and fate within the BWTF. The HIX and specific UV absorbance at 254 nm ($SUVA_{254}$) are optical parameters that serve as indicators of oxygenation and aromaticity, respectively (Gao et al. 2017; Hansen et al. 2016). Increasing HIX values indicate a rise in long-wavelength, oxygenated, and refractory compounds, while decreasing short-wavelength, labile compounds. Overall, HIX values show an increasing trend throughout the BWTF process (ρ = 0.693), ranging from 0.262 ± 0.013 (GS) to 0.376 ± 0.026 (DAF), indicating a compositional shift towards more oxygenated and complex compounds (Table S3). $SUVA_{254}$ tracks changes in HOPs by measuring the absorption of light by dissolved organic matter, with increasing values associated with higher aromaticity. In the BWTF process, $SUVA_{254}$

values decrease (ρ = -0.345), ranging from 0.008 ± 0.001 (Effluent) to 0.013 ± 0.001 (TP), indicating an overall decrease in aromaticity (Table S3). These observed HIX and $SUVA_{254}$ values align with previous studies characterizing laboratory-produced HOPs (Harsha et al. 2023; Whisenhant et al. 2022). Importantly, they are considerably lower than the values reported for coastal marine natural organic matter (HIX= ~4, $SUVA_{254}$=~3), indicating that the source of the dissolved organic matter in the BWTF is petroleum-derived HOPs rather than naturally derived compounds (D'Andrilli et al. 2022). These findings suggest a transformation of HOPs during the BWTF process, leading to an increase in oxygenation and complexity while exhibiting a slight decrease in aromaticity. This departure from the typical positive correlation between HIX and $SUVA_{254}$ highlights the complex nature of HOPs and emphasizes the necessity of employing multiple characterization techniques.

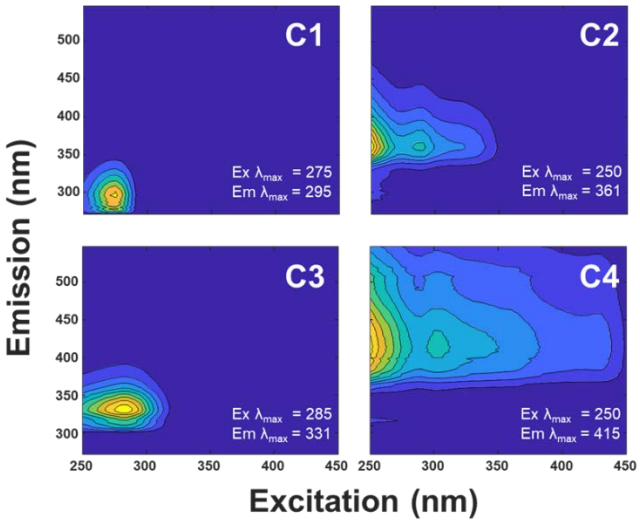

Figure 3. Validated four-component PARAFAC model.

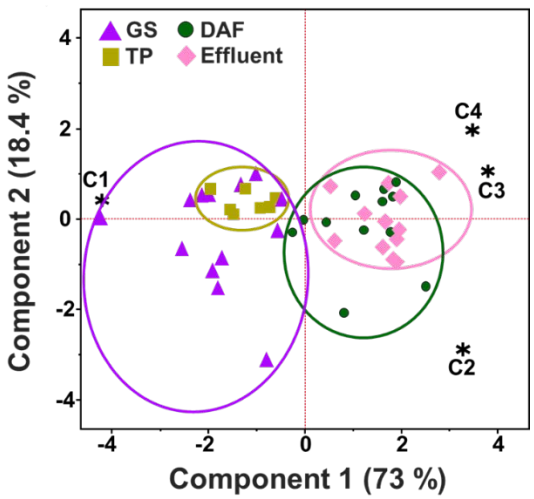

Figure 4. PCA biplot, loadings represent PARAFAC components.

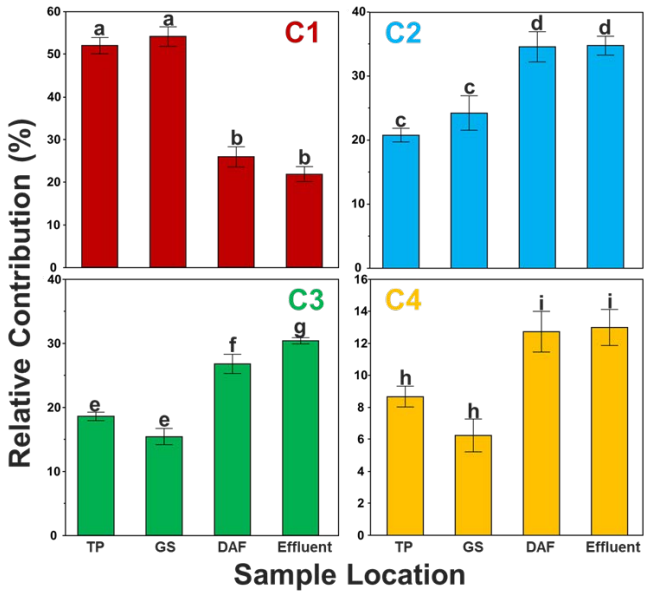

Figure 5. Relative contributions of PARAFAC components. Connecting letters for components are Student's t-test pairwise comparisons at 95% confidence.

PARAFAC was employed to investigate the underlying optical signatures in the EEMs dataset and track compositional changes during the BWTF process. A validated four-component PARAFAC model was derived (Figure 3). Each component corresponds to specific excitation and emission maxima (Ex/Em) values and exhibits distinct characteristics. Component 1 (C1)

has Ex/Em maxima at 275/295 nm and shows similarity to 15 entries (95-99% similarity score) in the OpenFluor database, which primarily characterizes natural organic matter (Graeber et al. 2012; Kowalczuk et al. 2013; Murphy et al. 2006; Osburn et al. 2016; D'Andrilli et al. 2017; Wheeler, Levia, and Hudson 2017; Painter et al. 2018; Yang et al. 2019; Sun et al. 2021; D'Andrilli et al. 2019; Chen et al. 2017; DeFrancesco and Guéguen 2021; Dall'Osto et al. 2022). This component is commonly referred to as a "protein-like" fluorescence signature in organic biogeochemistry, representing short-wavelength, reactive dissolved organic matter rather than actual proteins. In the context of HOPs, this signature indicates a composition of reduced, aliphatic, and low heteroatom structures, such as 3-ring alkylated and oxygenated PAHs. Component 2 (C2) with Ex/Em values of 250/361 nm matches seven published components (95-97% similarity), including two signatures derived from petroleum (Brünjes et al. 2022; Catalán et al. 2021; Retelletti Brogi, Kim, et al. 2019; Podgorski et al. 2018; Bittar et al. 2016; Williams et al. 2010; Murphy et al. 2013). One match is found in a study by Podgorski et al., which investigated petroleum-contaminated groundwater and identified biorefractory HOPs composed of low molecular weight, highly aromatic, and oxygenated compounds (Podgorski et al. 2018). The second match is found in a study by Brünjes et al., focusing on the biodegradation of asphaltenes through laboratory incubations, representing another potential biorefractory signature (Brünjes et al. 2022). Component 3 (C3) with Ex/Em values of 285/331 nm matches 22 published components (96-99% similarity), three of which are petroleum-derived (Harsha et al. 2023; Sheng et al. 2021; Gao and Guéguen 2017; DeFrancesco and Guéguen 2021; Retelletti Brogi et al. 2022; Brünjes et al. 2022; Wünsch and Murphy 2021; Batista-Andrade et al. 2023; Retelletti Brogi et al. 2020; Lee et al. 2018; Kim et al. 2022; Retelletti Brogi, Jung, et al. 2019; D'Andrilli et al. 2019; Yamashita et al. 2011; Stedmon and Markager 2005; Yu et al. 2015; Murphy et al. 2011; Hambly et al. 2015; Cawley, Butler, et al. 2012; Cawley, Ding, et al. 2012; Podgorski et al. 2018). C3 aligns with C5 in the groundwater study by Podgorski et al., representing short-wavelength, polynuclear PAHs that are biolabile and acutely toxic HOPs (Podgorski et al. 2018). C3 also matches with C3 in the asphaltene biodegradation study by Brünjes et al., indicating biolabile and potentially toxic HOPs(Brünjes et al. 2022). Furthermore, C3 matches with C4 in a previous study by

Harsha et al., which characterized photoproduced HOPs in laboratory simulations, representing reduced, aliphatic HOPs generated from 24-hour irradiated diesel (Harsha et al. 2023). Component 4 (C4) has Ex/Em values of 250/415 nm and matches 11 published models, including two unique petroleum signatures (Huang et al. 2022; Brünjes et al. 2022; Jeon et al. 2021; Lin and Guo 2020; Whisenhant et al. 2022; Cabrera et al. 2020; Jia et al. 2017; Chen et al. 2017; D'Andrilli et al. 2019; Painter et al. 2018; Retelletti Brogi et al. 2018). C4 corresponds to C4 in the asphaltene biodegradation study by Brünjes et al., exhibiting a "humic-like" fluorescence signature (Brünjes et al. 2022). C4 also matches with C1 in a study by Whisenhant et al. examining photoproduced HOPs generated from laboratory simulations, where C1 represented the most degraded HOPs that exhibited "humic-like" fluorescence (Whisenhant et al. 2022). This result indicates the presence of HOPs composed of long-wavelength, aromatic, oxygenated, and heteroatomic compounds. Three out of the four components identified in the PARAFAC analysis align with components from the Brünjes et al. study, suggesting that the optical signatures measured in the BWTF process are likely petroleum-derived (Brünjes et al. 2022). Overall, the HOPs associated with the BWTF process range from short-wavelength (aliphatic, reduced, biolabile) to long-wavelength (aromatic, oxygenated, refractory) compounds, with the order of increasing wavelength being C1 > C3 > C2 > C4.

Principal component analysis (PCA) illustrates the relationship between each component and the treatment process (Figure 4). C1 exhibits a close association with TP and GS, while C2 is linked to the DAF process. C3 and C4 represent the effluent. Overall, PCA reveals similarities between TP and GS, as well as between DAF and effluent. By measuring the relative contribution of each optical signature, the compositional changes resulting from the BWTF process are uncovered (Figure 5). There are no significant differences in component contribution between TP and GS, as well as between DAF and effluent, except for C3. This finding indicates that C3 undergoes significant transformation during the BT process. Notably, C1 is the only signature that decreases due to the BWTF process ($\rho = -0.805$). This correlation suggests that the short-wavelength HOPs represented by C1 are labile and

undergo substantial oxidation during the DAF process, resulting in a ~52% reduction in the C1 signature between GS and DAF. On the other hand, C2, C3, and C4 increase with the BWTF process (ρ = 0.713, 0.453, and 0.544, respectively), indicating the oxidation process leading to varying types of HOPs. After the DAF process, C2 shows an increase of ~43%, which is the smallest transformation observed among the components coupled and no compositional change due to BT. This result suggests that C2 may represent more refractory HOPs, as also noted in the matched components in the studies by Podgorski et al. and Brünjes et al., indicating its potential use for oil treatment and spill monitoring (Brünjes et al. 2022; Podgorski et al. 2018). C3 experiences a significant increase of ~74% after DAF and is the only signature significantly changed due to BT, with an increase of ~13%. This highlights the biolabile nature of C3, which has been identified as a significant driver of acute toxicity in the matched studies. It constitutes ~30% of the optical signatures observed in the effluent and increases with biological treatment. C4 exhibits an increase of ~104% after DAF treatment and represents the most aromatic and oxygenated signature, reflecting the most degraded HOPs in the BWTF process. Overall, C4 constitutes approximately 10% of the total observed signatures at the BWTF, suggesting that the BWTF process does not significantly degrade HOPs into these long-wavelength compounds. Instead, semi-labile/labile HOPs are released into the aquatic ecosystem, posing a higher likelihood of reactivity and potential effects in aquatic ecosystems.

3.3. Trends in HM concentrations

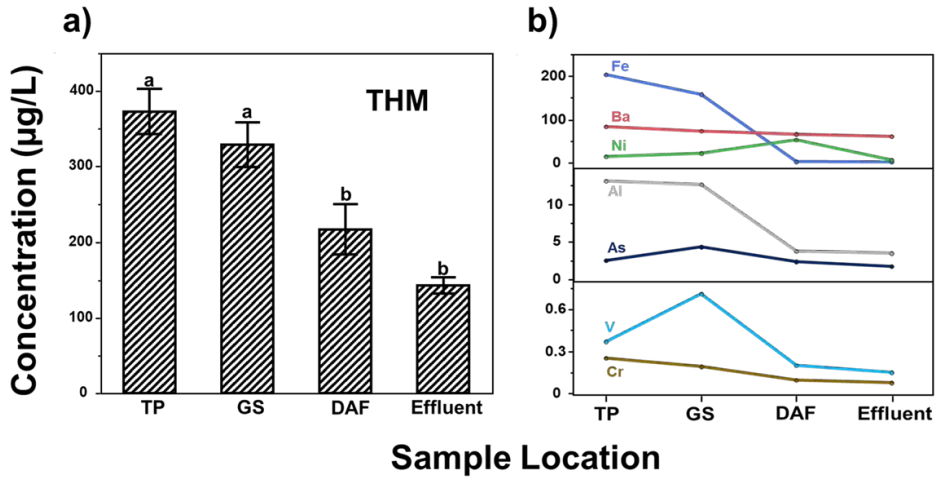

Figure 6. Shifts in (a) total and (b) significant HMs through the treatment process. Error bars are removed from significant HMs plot for clear visualization. Connecting letters for THM are Student's t-test pairwise comparisons at 95% confidence.

The BWTF process significantly affects the concentration of HMs in oiled ballast water, as revealed by a large quantitative screening. Overall, the total concentration of heavy metals (THM) decreases significantly with the BWTF process, and similar trends are observed as with HOPs. The only significant transformation occurs during the DAF process (ρ = -0.814) (Figure 6a). After the DAF process, the THM concentration decreases by approximately 34%. The measured THM concentrations throughout the BWTF process range from 143 ± 11.0 (effluent) to 373 ± 29.7 µg/L (TP).

Out of the 18 HMs measured, only seven show significant trends with the BWTF process, and all exhibit negative correlations (Table S4). These significant metals are divided into three concentration levels: high (1.5 – 203 µg/L) including Fe, Ba, and Ni; medium (1.5 – 13.1 µg/L) including Al and As; and low (0.148 – 2.02 µg/L) including V and Cr (Figure 6b). Of particular interest is zinc (Zn), which ADEC categorizes as a parameter of concern and is believed to be the main driver of effluent toxicity. The Zn concentrations in this study range from 30.1 ± 0.139 (TP) to 31.4 ± 0.150 µg/L (DAF), which are significantly lower than the permit-set limit

for effluent (4,150 µg/L) and the water quality standard limit (86.14 µg/L). The measured effluent Zn concentrations from 2008 to 2017 range from 53 to 1,450 µg/L, with an average of 267 µg/L, which is approximately 8.5 times higher than the reported values from this study.

Possible sources of HMs in the oiled ballast water include interactions with metal industrial equipment and from crude oil (Chinedu and Chukwuemeka 2018; Ajeel et al. 2021; ADEC 2019). None of the measured HMs exceeded the water quality standards set by ADEC and the EPA (ADEC 2019). However, a potential threat associated with the discharge of HMs from the BWTF is their sorption and accumulation in sediment, which poses an ecological risk (Zhao et al. 2021; Iordache et al. 2022; Miranda et al. 2022).

3.4. Comparison between stormwater and oiled ballast water

The unexpected similarities between TP (assumed stormwater) and GS (gravity separation tank) in terms of measured contaminants (HOPs and HMs) raise questions about the assumption that TP is a non-contaminated water source and its capacity to dilute oiled ballast water. Surprisingly, all the measured data quantifying and characterizing HOPs and HMs were statistically insignificant. This finding challenges the belief that TP, based on historical contribution data, is a non-contaminated water source that dilutes contaminants from oiled ballast water.

Recorded values from the gravity separation tank before and after ballast offloading indicate an average dilution factor of 44:1 for oiled ballast water. Considering this dilution factor, the expected concentrations and composition of contaminants (HOPs and HMs) were anticipated to be low in TP. However, the actual measurements did not align with these expectations. Previous monitoring data reported very low levels (below detection limits) of BTEX, suggesting that TP is not contaminated and likely dilutes the contaminants in oiled ballast water (ADEC 2019). Based on these reports, the NVDOC values in TP samples were expected to be lower. However, the measured NVDOC concentrations suggest that the stormwater may contain hydrocarbons that are not detected by BTEX measurements.

Furthermore, the optical signatures indicate that the source of dissolved organic matter is derived from petroleum rather than naturally occurring substances.

This observed relationship could be attributed to various factors, such as residual oil contamination during the industrial process, higher levels of industrial waste influent, or contaminated stormwater itself. Further study and monitoring are necessary to gain valuable insight into the sources of contaminants being treated at the BWTF. Understanding the composition of the other influents is of utmost importance, especially considering that ADEC permits the discharge of untreated stormwater during periods of high rainfall.

3.5. Implications for environmental monitoring

This study utilized a wide range of analytical techniques to investigate the BWTF process in greater detail, uncovering previously undetected contaminants. The findings indicate that the BWTF effectively removes BTEX from oiled ballast water but fails to remove HOPs. Instead, the process generates and releases a diverse range of compositionally complex HOPs, which may pose ecological risks. The C3 optical signature identified in this study matched with other published components known to exhibit acute toxicity.

The toxicity mechanism of HOPs in the environment is not well understood, but existing literature suggests that HOPs may be more toxic than their parent petroleum compounds due to increased bioavailability resulting from higher oxygen content.(Katz et al. 2022) Although the measured levels of HOPs and HMs in the effluent are not alarmingly high, it is crucial to consider the volume of effluent being discharged into Port Valdez, which averages 1.72 million gallons per day (ADEC 2019). When normalized, this study reveals that 15 kilograms (kg) of HOPs and 11 grams (g) of arsenic are released into the water daily during the processing of oiled ballast water. These significant quantities have the potential to enter the aquatic ecosystem, transport through the water column, bioaccumulate in organisms, and sorb into sediment, posing potential harm over time.

The techniques employed in this study, such as NVDOC and optical analyses, have the potential to be used as broad monitoring tools for oil contamination. NVDOC provides a comprehensive quantification of dissolved organic carbon from oiled ballast water, going beyond specific fractions like BTEX or TAqH, thus offering insights into the carbon release. Additionally, optical signatures can characterize general qualities such as reactivity, aromaticity, and oxygen content. Utilizing remote fluorescence sensors calibrated with petroleum-specific signatures may enable monitoring the formation and transport of HOPs in the BWTF. Adequate monitoring in oiled ballast water treatment is essential for understanding the release and transport of contaminants into the environment.

Associated Content:

Supporting Information

ICP-QQQ operating conditions; ICP-QQQ specific analyte information; HOPs characterization data; metric correlations; HM concentration levels (PDF)

Conflict of Interest:

The authors declare no competing financial interest.

Acknowledgements:

Research supported by the Prince William Sound Regional Citizens' Advisory Council (PWSRCAC). M.L. Harsha was partially supported by an Oil Spill Recovery Institute Graduate Research Fellowship (22-10-09). ICP-QQQ was awarded through an NSF MRI CHE2018417. A special thank you to Austin Love at PWSRCAC for the helpful guidance and information. Thanks to Sheila Mann and the Analytical Services Laboratory team at Alyeska Pipeline Service Company for coordination, sample collection, and BTEX analysis.

References:

ADEC, Alaska Department of Environmental Conservation. 2019. "ALASKA POLLUTANT DISCHARGE ELIMINATION SYSTEM PERMIT - Alyeska Pipeline Service Company, Valdez Marine Terminal." In *AK0023248*, edited by Alaska Department of Environmental Conservation.

Aeppli, Christoph, Catherine A. Carmichael, Robert K. Nelson, Karin L. Lemkau, William M. Graham, Molly C. Redmond, David L. Valentine, and Christopher M. Reddy. 2012. 'Oil Weathering after the Deepwater Horizon Disaster Led to the Formation of Oxygenated Residues', *Environmental Science & Technology*, 46: 8799-807.

Ajeel, M. A., A. A. Ajeel, A. M. Nejres, and R. A. Salih. 2021. 'Assessment of Heavy Metals and Related Impacts on Antioxidants and Physiological Parameters in Oil Refinery Workers in Iraq', *J Health Pollut*, 11: 210907.

Batista-Andrade, Jahir A., Erick Diaz, Diego Iglesias Vega, Ethan Hain, Michael R. Rose, and Lee Blaney. 2023. 'Spatiotemporal analysis of fluorescent dissolved organic matter to identify the impacts of failing sewer infrastructure in urban streams', *Water Research*, 229: 119521.

Bittar, Thais B., Stella A. Berger, Laura M. Birsa, Tina L. Walters, Megan E. Thompson, Robert G. M. Spencer, Elizabeth L. Mann, Aron Stubbins, Marc E. Frischer, and Jay A. Brandes. 2016. 'Seasonal dynamics of dissolved, particulate and microbial components of a tidal saltmarsh-dominated estuary under contrasting levels of freshwater discharge', *Estuarine, Coastal and Shelf Science*, 182: 72-85.

Boduszynski, Mieczyslaw M. 1987. 'Composition of heavy petroleums. 1. Molecular weight, hydrogen deficiency, and heteroatom concentration as a function of atmospheric equivalent boiling point up to 1400.degree.F (760.degree.C)', *Energy & Fuels*, 1: 2-11.

———. 1988. 'Composition of heavy petroleums. 2. Molecular characterization', *Energy & Fuels*, 2: 597-613.

Boduszynski, Mieczyslaw M., and Klaus H. Altgelt. 1992. 'Composition of heavy petroleums. 4. Significance of the extended atmospheric equivalent boiling point (AEBP) scale', *Energy & Fuels*, 6: 72-76.

Brünjes, Jonas, Michael Seidel, Thorsten Dittmar, Jutta Niggemann, and Florence Schubotz. 2022. 'Natural Asphalt Seeps Are Potential Sources for Recalcitrant Oceanic Dissolved Organic Sulfur and Dissolved Black Carbon', *Environmental Science & Technology*, 56: 9092-102.

Cabrera, J. M., P. E. García, F. L. Pedrozo, and C. P. Queimaliños. 2020. 'Dynamics of the dissolved organic matter in a stream-lake system within an extremely acid to neutral pH range: Agrio-Caviahue watershed', *Spectrochimica Acta Part A: Molecular and Biomolecular Spectroscopy*, 235: 118278.

Catalán, Núria, Ada Pastor, Carles M. Borrego, Joan Pere Casas-Ruiz, Jeffrey A. Hawkes, Carmen Gutiérrez, Daniel von Schiller, and Rafael Marcé. 2021. 'The relevance of environment vs. composition on dissolved organic matter degradation in freshwaters', *Limnology and Oceanography*, 66: 306-20.

Cawley, Kaelin M., Kenna D. Butler, George R. Aiken, Laurel G. Larsen, Thomas G. Huntington, and Diane M. McKnight. 2012. 'Identifying fluorescent pulp mill effluent in the Gulf of Maine and its watershed', *Marine Pollution Bulletin*, 64: 1678-87.

Cawley, Kaelin M., Yan Ding, James Fourqurean, and Rudolf Jaffé. 2012. 'Characterising the sources and fate of dissolved organic matter in Shark Bay, Australia: a preliminary study using optical properties and stable carbon isotopes', *Marine and Freshwater Research*, 63: 1098-107.

Chen, Meilian, Sung-Han Kim, Heon-Jae Jung, Jung-Ho Hyun, Jung Hyun Choi, Hyo-Jin Lee, In-Ae Huh, and Jin Hur. 2017. 'Dynamics of dissolved organic matter in riverine sediments affected by weir impoundments: Production, benthic flux, and environmental implications', *Water Research*, 121: 150-61.

Chinedu, E., and C. K. Chukwuemeka. 2018. 'Oil Spillage and Heavy Metals Toxicity Risk in the Niger Delta, Nigeria', *J Health Pollut*, 8: 180905.

D'Andrilli, J., C. M. Foreman, M. Sigl, J. C. Priscu, and J. R. McConnell. 2017. 'A 21 000-year record of fluorescent organic matter markers in the WAIS Divide ice core', *Clim. Past*, 13: 533-44.

D'Andrilli, Juliana, James R. Junker, Heidi J. Smith, Eric A. Scholl, and Christine M. Foreman. 2019. 'DOM composition alters ecosystem function during microbial processing of isolated sources', *Biogeochemistry*, 142: 281-98.

D'Andrilli, Juliana, Victoria Silverman, Shelby Buckley, and Fernando L. Rosario-Ortiz. 2022. 'Inferring Ecosystem Function from Dissolved Organic Matter Optical Properties: A Critical Review', *Environmental Science & Technology*, 56: 11146-61.

D'Auria, Maurizio, Lucia Emanuele, Rocco Racioppi, and Vincenzina Velluzzi. 2009. 'Photochemical degradation of crude oil: Comparison between direct irradiation, photocatalysis, and photocatalysis on zeolite', *Journal of Hazardous Materials*, 164: 32-38.

Dall'Osto, Manuel, Dolors Vaqué, Ana Sotomayor-Garcia, Miguel Cabrera-Brufau, Marta Estrada, Teresa Buchaca, Montserrat Soler, Sdena Nunes, Sebastian Zeppenfeld, Manuela van Pinxteren, Hartmut Herrmann, Heike Wex, Matteo Rinaldi, Marco Paglione, David C. S. Beddows, Roy M. Harrison, and Elisa Berdalet. 2022. 'Sea Ice Microbiota in the Antarctic Peninsula Modulates Cloud-Relevant Sea Spray Aerosol Production', *Frontiers in Marine Science*, 9.

DeFrancesco, C., and C. Guéguen. 2021. 'Long-term Trends in Dissolved Organic Matter Composition and Its Relation to Sea Ice in the Canada Basin, Arctic Ocean (2007–2017)', *Journal of Geophysical Research: Oceans*, 126: e2020JC016578.

Farrington, John, and James Quinn. 2015. '"Unresolved Complex Mixture" (UCM): A brief history of the term and moving beyond it', *Marine Pollution Bulletin*, 96.

Freeman, Danielle Haas, and Collin P. Ward. 2022. 'Sunlight-driven dissolution is a major fate of oil at sea', *Science Advances*, 8: eabl7605.

Fry, N., and R. A. Steenson. 2019. 'User's Guide: Derivation and Application of Environmental Screening Levels (ESLs)', *San Francisco Bay Regional Water Quality Control Board: San Fransisco*: 1-35.

Frysinger, Glenn S., Richard B. Gaines, Li Xu, and Christopher M. Reddy. 2003. 'Resolving the Unresolved Complex Mixture in Petroleum-Contaminated Sediments', *Environmental Science & Technology*, 37: 1653-62.

Gao, Jiakai, Chenglong Liang, Guangzhu Shen, Jialong Lv, and Haiming Wu. 2017. 'Spectral characteristics of dissolved organic matter in various agricultural soils throughout China', *Chemosphere*, 176: 108-16.

Gao, Zhiyuan, and Céline Guéguen. 2017. 'Size distribution of absorbing and fluorescing DOM in Beaufort Sea, Canada Basin', *Deep Sea Research Part I: Oceanographic Research Papers*, 121: 30-37.

Graeber, Daniel, Jörg Gelbrecht, Martin T. Pusch, Christine Anlanger, and Daniel von Schiller. 2012. 'Agriculture has changed the amount and composition of dissolved organic matter in Central European headwater streams', *Science of The Total Environment*, 438: 435-46.

Hambly, A. C., E. Arvin, L. F. Pedersen, P. B. Pedersen, B. Seredyńska-Sobecka, and C. A. Stedmon. 2015. 'Characterising organic matter in recirculating aquaculture systems with fluorescence EEM spectroscopy', *Water Research*, 83: 112-20.

Hansen, Angela, Tamara E. C. Kraus, Brian Pellerin, Jacob Fleck, Bryan D. Downing, and Brian A. Bergamaschi. 2016. 'Optical properties of dissolved organic matter (DOM):

Effects of biological and photolytic degradation', *Limnology and Oceanography*, 61: 1015-32.

Harsha, Maxwell L., Zachary C. Redman, Josh Wesolowski, David C. Podgorski, and Patrick L. Tomco. 2023. 'Photochemical formation of water-soluble oxyPAHs, naphthenic acids, and other hydrocarbon oxidation products from Cook Inlet, Alaska crude oil and diesel in simulated seawater spills', *Environmental Science: Advances*, 2: 447-61.

Harshman, Richard A., and Margaret E. Lundy. 1994. 'PARAFAC: Parallel factor analysis', *Computational Statistics & Data Analysis*, 18: 39-72.

Hollebone, B. 2011. 'Measurement of Oil Physical Properties.' in.

Huang, Xian, Caixia Yan, Minghua Nie, Jie Chen, and Mingjun Ding. 2022. 'Effect of colloidal fluorescence properties on the complexation of chloramphenicol and carbamazepine to the natural aquatic colloids', *Chemosphere*, 286: 131604.

Iordache, A. M., C. Nechita, R. Zgavarogea, C. Voica, M. Varlam, and R. E. Ionete. 2022. 'Accumulation and ecotoxicological risk assessment of heavy metals in surface sediments of the Olt River, Romania', *Sci Rep*, 12: 880.

Jeon, Mi Hae, Jinyoung Jung, Mi Ok Park, Shigeru Aoki, Tae-Wan Kim, and Seung-Kyu Kim. 2021. 'Tracing Circumpolar Deep Water and glacial meltwater using humic-like fluorescent dissolved organic matter in the Amundsen Sea, Antarctica', *Marine Chemistry*, 235: 104008.

Jia, Fangxu, Qing Yang, Xiuhong Liu, Xiyao Li, Baikun Li, Liang Zhang, and Yongzhen Peng. 2017. 'Stratification of Extracellular Polymeric Substances (EPS) for Aggregated Anammox Microorganisms', *Environmental Science & Technology*, 51: 3260-68.

Katz, Samuel, Haining Chen, David Fields, Erin Beirne, Phoebe Keyes, Greg Drozd, and Christoph Aeppli. 2022. *Changes in chemical composition and copepod toxicity during petroleum photooxidation*.

Kim, Jeonghyun, Yeseul Kim, Sung Eun Park, Tae-Hoon Kim, Bong-Guk Kim, Dong-Jin Kang, and TaeKeun Rho. 2022. 'Impact of aquaculture on distribution of dissolved organic matter in coastal Jeju Island, Korea, based on absorption and fluorescence spectroscopy', *Environmental Science and Pollution Research*, 29: 553-63.

Kowalczuk, Piotr, Gavin H. Tilstone, Monika Zabłocka, Rüdiger Röttgers, and Rob Thomas. 2013. 'Composition of dissolved organic matter along an Atlantic Meridional Transect from fluorescence spectroscopy and Parallel Factor Analysis', *Marine Chemistry*, 157: 170-84.

Krajewski, Logan C., Ryan P. Rodgers, and Alan G. Marshall. 2017. '126 264 Assigned Chemical Formulas from an Atmospheric Pressure Photoionization 9.4 T Fourier Transform Positive Ion Cyclotron Resonance Mass Spectrum', *Analytical Chemistry*, 89: 11318-24.

Kubota, Tetsuo 2022. "Analysis of Undiluted Seawater using ICP-MS with Ultra High Matrix Introduction and Discrete Sampling " In. Agilent Application Note: Agilent Technologies.

Kurniawan, Setyo Budi, Dwi Sasmita Aji Pambudi, Mahasin Maulana Ahmad, Benedicta Dian Alfanda, Muhammad Fauzul Imron, and Siti Rozaimah Sheikh Abdullah. 2022. 'Ecological impacts of ballast water loading and discharge: insight into the toxicity and accumulation of disinfection by-products', *Heliyon*, 8: e09107.

Lamoureux, Vincent B, and World Health Organization. 1967. *Guide to ship sanitation* (World Health Organization).

Lee, Doorae, Minhwan Kwon, Yongtae Ahn, Youmi Jung, Seong-Nam Nam, Il-hwan Choi, and Joon-Wun Kang. 2018. 'Characteristics of intracellular algogenic organic matter and its reactivity with hydroxyl radicals', *Water Research*, 144: 13-25.

Lin, Hui, and Laodong Guo. 2020. 'Variations in Colloidal DOM Composition with Molecular Weight within Individual Water Samples as Characterized by Flow Field-Flow Fractionation and EEM-PARAFAC Analysis', *Environmental Science & Technology*, 54: 1657-67.

Little, Edward, Laverne Cleveland, Robin Calfee, and Mace Barron. 2000. 'Assessment of the photoenhanced toxicity of a weathered oil to the tidewater silverside', *Environmental Toxicology and Chemistry*, 19: 926-32.

Love, Austin. 2018. "2013-2017 Valdez Marine Terminal Water Quality Data Review." In.

Maki, H., T. Sasaki, and S. Harayama. 2001. 'Photo-oxidation of biodegraded crude oil and toxicity of the photo-oxidized products', *Chemosphere*, 44: 1145-51.

McKenna, Amy M., Robert K. Nelson, Christopher M. Reddy, Joshua J. Savory, Nathan K. Kaiser, Jade E. Fitzsimmons, Alan G. Marshall, and Ryan P. Rodgers. 2013. 'Expansion of the Analytical Window for Oil Spill Characterization by Ultrahigh Resolution Mass Spectrometry: Beyond Gas Chromatography', *Environmental Science & Technology*, 47: 7530-39.

Miranda, Lorena S., Godwin A. Ayoko, Prasanna Egodawatta, and Ashantha Goonetilleke. 2022. 'Adsorption-desorption behavior of heavy metals in aquatic environments: Influence of sediment, water and metal ionic properties', *Journal of Hazardous Materials*, 421: 126743.

Murphy, Kathleen R., Adam Hambly, Sachin Singh, Rita K. Henderson, Andy Baker, Richard Stuetz, and Stuart J. Khan. 2011. 'Organic Matter Fluorescence in Municipal Water Recycling Schemes: Toward a Unified PARAFAC Model', *Environmental Science & Technology*, 45: 2909-16.

Murphy, Kathleen R., Gregory M. Ruiz, William T. M. Dunsmuir, and T. David Waite. 2006. 'Optimized Parameters for Fluorescence-Based Verification of Ballast Water Exchange by Ships', *Environmental Science & Technology*, 40: 2357-62.

Murphy, Kathleen R., Colin A. Stedmon, Daniel Graeber, and Rasmus Bro. 2013. 'Fluorescence spectroscopy and multi-way techniques. PARAFAC', *Analytical Methods*, 5: 6557-66.

Murphy, Kathleen R., Colin A. Stedmon, Philip Wenig, and Rasmus Bro. 2014. 'OpenFluor– an online spectral library of auto-fluorescence by organic compounds in the environment', *Analytical Methods*, 6: 658-61.

Ohno, Tsutomu. 2002. 'Fluorescence Inner-Filtering Correction for Determining the Humification Index of Dissolved Organic Matter', *Environmental Science & Technology*, 36: 742-46.

Osburn, Christopher L., Lauren T. Handsel, Benjamin L. Peierls, and Hans W. Paerl. 2016. 'Predicting Sources of Dissolved Organic Nitrogen to an Estuary from an Agro-Urban Coastal Watershed', *Environmental Science & Technology*, 50: 8473-84.

Painter, Stuart C., Dan J. Lapworth, E. Malcolm S. Woodward, Silke Kroeger, Chris D. Evans, Daniel J. Mayor, and Richard J. Sanders. 2018. 'Terrestrial dissolved organic matter distribution in the North Sea', *Science of The Total Environment*, 630: 630-47.

Palacio Lozano, Diana Catalina, Remy Gavard, Juan P. Arenas-Diaz, Mary J. Thomas, David D. Stranz, Enrique Mejía-Ospino, Alexander Guzman, Simon E. F. Spencer, David Rossell, and Mark P. Barrow. 2019. 'Pushing the analytical limits: new insights into complex mixtures using mass spectra segments of constant ultrahigh resolving power', *Chemical Science*, 10: 6966-78.

Park, Ji Won, Sang Yeob Kim, Jin Hyung Noh, Young Ho Bae, Jae Woo Lee, and Sung Kyu Maeng. 2022. 'A shift from chemical oxygen demand to total organic carbon for stringent industrial wastewater regulations: Utilization of organic matter characteristics', *Journal of Environmental Management*, 305: 114412.

Payne, James, William Driskell, Joan Braddock, and Justin Bailey. 2005. 'Hydrocarbon Biodegradation in the Ballast Water Treatment Facility, Alyeska Marine Terminal'.

Podgorski, David C., Phoebe Zito, Jennifer T. McGuire, Dalma Martinovic-Weigelt, Isabelle M. Cozzarelli, Barbara A. Bekins, and Robert G. M. Spencer. 2018. 'Examining Natural

Attenuation and Acute Toxicity of Petroleum-Derived Dissolved Organic Matter with Optical Spectroscopy', *Environmental Science & Technology*, 52: 6157-66.

Proper, Wim, Ed Mccurdy, and Jun-ichi Takahashi. 2020. "Performance of the Agilent 7900 ICP-MS with UHMI for High Salt Matrix Analysis." In. Agilent Application Note: Agilent Technologies.

Ray, Phoebe Z., Huan Chen, David C. Podgorski, Amy M. McKenna, and Matthew A. Tarr. 2014. 'Sunlight creates oxygenated species in water-soluble fractions of Deepwater horizon oil', *Journal of Hazardous Materials*, 280: 636-43.

Retelletti Brogi, S., G. Cossarini, G. Bachi, C. Balestra, E. Camatti, R. Casotti, G. Checcucci, S. Colella, V. Evangelista, F. Falcini, F. Francocci, T. Giorgino, F. Margiotta, M. Ribera d'Alcalà, M. Sprovieri, S. Vestri, and C. Santinelli. 2022. 'Evidence of Covid-19 lockdown effects on riverine dissolved organic matter dynamics provides a proof-of-concept for needed regulations of anthropogenic emissions', *Science of The Total Environment*, 812: 152412.

Retelletti Brogi, Simona, Cecilia Balestra, Raffaella Casotti, Gianpiero Cossarini, Yuri Galletti, Margherita Gonnelli, Stefano Vestri, and Chiara Santinelli. 2020. 'Time resolved data unveils the complex DOM dynamics in a Mediterranean river', *Science of The Total Environment*, 733: 139212.

Retelletti Brogi, Simona, Sun-Yong Ha, Kwanwoo Kim, Morgane Derrien, Yun Kyung Lee, and Jin Hur. 2018. 'Optical and molecular characterization of dissolved organic matter (DOM) in the Arctic ice core and the underlying seawater (Cambridge Bay, Canada): Implication for increased autochthonous DOM during ice melting', *Science of The Total Environment*, 627: 802-11.

Retelletti Brogi, Simona, Jin Young Jung, Sun-Yong Ha, and Jin Hur. 2019. 'Seasonal differences in dissolved organic matter properties and sources in an Arctic fjord: Implications for future conditions', *Science of The Total Environment*, 694: 133740.

Retelletti Brogi, Simona, Ji-Hoon Kim, Jong-Sik Ryu, Young Keun Jin, Yun Kyung Lee, and Jin Hur. 2019. 'Exploring sediment porewater dissolved organic matter (DOM) in a mud volcano: Clues of a thermogenic DOM source from fluorescence spectroscopy', *Marine Chemistry*, 211: 15-24.

Sheng, Yanru, Caixia Yan, Minghua Nie, Min Ju, Mingjun Ding, Xian Huang, and Jiaming Chen. 2021. 'The partitioning behavior of PAHs between settled dust and its extracted water phase: Coefficients and effects of the fluorescent organic matter', *Ecotoxicology and Environmental Safety*, 223: 112573.

Spencer, R. G., L. Bolton, and A. Baker. 2007. 'Freeze/thaw and pH effects on freshwater dissolved organic matter fluorescence and absorbance properties from a number of UK locations', *Water Res*, 41: 2941-50.

Stedmon, Colin A., and Rasmus Bro. 2008. 'Characterizing dissolved organic matter fluorescence with parallel factor analysis: a tutorial', *Limnology and Oceanography: Methods*, 6: 572-79.

Stedmon, Colin A., and Stiig Markager. 2005. 'Tracing the production and degradation of autochthonous fractions of dissolved organic matter by fluorescence analysis', *Limnology and Oceanography*, 50: 1415-26.

Stubbins, Aron, and Thorsten Dittmar. 2012. 'Low volume quantification of dissolved organic carbon and dissolved nitrogen', *Limnology and Oceanography: Methods*, 10: 347-52.

Sun, Yuqin, Kale Clauson, Min Zhou, Ziyong Sun, Chunmiao Zheng, and Yan Zheng. 2021. 'Hillslopes in Headwaters of Qinghai-Tibetan Plateau as Hotspots for Subsurface Dissolved Organic Carbon Processing During Permafrost Thaw', *Journal of Geophysical Research: Biogeosciences*, 126: e2020JG006222.

Tfaily, M. M., D. C. Podgorski, J. E. Corbett, J. P. Chanton, and W. T. Cooper. 2011. 'Influence of acidification on the optical properties and molecular composition of dissolved organic matter', *Anal Chim Acta*, 706: 261-7.

Verna, Danielle E., and Bradley P. Harris. 2016. 'Review of ballast water management policy and associated implications for Alaska', *Marine Policy*, 70: 13-21.

Ward, Collin P., and Edward B. Overton. 2020. 'How the 2010 Deepwater Horizon spill reshaped our understanding of crude oil photochemical weathering at sea: a past, present, and future perspective', *Environmental Science: Processes & Impacts*, 22: 1125-38.

Ward, Collin P., Charles M. Sharpless, David L. Valentine, Deborah P. French-McCay, Christoph Aeppli, Helen K. White, Ryan P. Rodgers, Kelsey M. Gosselin, Robert K. Nelson, and Christopher M. Reddy. 2018. 'Partial Photochemical Oxidation Was a Dominant Fate of Deepwater Horizon Surface Oil', *Environmental Science & Technology*, 52: 1797-805.

Wheeler, K. I., D. F. Levia, and J. E. Hudson. 2017. 'Tracking senescence-induced patterns in leaf litter leachate using parallel factor analysis (PARAFAC) modeling and self-organizing maps', *Journal of Geophysical Research: Biogeosciences*, 122: 2233-50.

Whisenhant, Elizabeth A., Phoebe Zito, David C. Podgorski, Amy M. McKenna, Zachary C. Redman, and Patrick L. Tomco. 2022. 'Unique Molecular Features of Water-Soluble

Photo-Oxidation Products among Refined Fuels, Crude Oil, and Herded Burnt Residue under High Latitude Conditions', *ACS ES&T Water*, 2: 994-1002.

Williams, Clayton J., Youhei Yamashita, Henry F. Wilson, Rudolf Jaffé, and Marguerite A. Xenopoulos. 2010. 'Unraveling the role of land use and microbial activity in shaping dissolved organic matter characteristics in stream ecosystems', *Limnology and Oceanography*, 55: 1159-71.

Wünsch, Urban J., and Kathleen Murphy. 2021. 'A simple method to isolate fluorescence spectra from small dissolved organic matter datasets', *Water Research*, 190: 116730.

Yamashita, Youhei, Anouska Panton, Claire Mahaffey, and Rudolf Jaffé. 2011. 'Assessing the spatial and temporal variability of dissolved organic matter in Liverpool Bay using excitation–emission matrix fluorescence and parallel factor analysis', *Ocean Dynamics*, 61: 569-79.

Yan, Mingquan, Qiangwei Fu, Dechao Li, Gunfa Gao, and Dongsheng Wang. 2013. 'Study of the pH influence on the optical properties of dissolved organic matter using fluorescence excitation–emission matrix and parallel factor analysis', *Journal of Luminescence*, 142: 103-09.

Yang, Liyang, Qiong Cheng, Wan- E. Zhuang, Hui Wang, and Wei Chen. 2019. 'Seasonal changes in the chemical composition and reactivity of dissolved organic matter at the land-ocean interface of a subtropical river', *Environmental Science and Pollution Research*, 26: 24595-608.

Yang, Liyang, Dae Ho Han, Bo-Mi Lee, and Jin Hur. 2015. 'Characterizing treated wastewaters of different industries using clustered fluorescence EEM–PARAFAC and FT-IR spectroscopy: Implications for downstream impact and source identification', *Chemosphere*, 127: 222-28.

Yu, Huarong, Heng Liang, Fangshu Qu, Zheng-shuang Han, Senlin Shao, Haiqing Chang, and Guibai Li. 2015. 'Impact of dataset diversity on accuracy and sensitivity of parallel factor analysis model of dissolved organic matter fluorescence excitation-emission matrix', *Scientific Reports*, 5: 10207.

Zhao, Yanqi, Ying Yang, Rongkun Dai, Sobkowiak Leszek, Xinyi Wang, and Lizhi Xiao. 2021. 'Adsorption and migration of heavy metals between sediments and overlying water in the Xinhe River in central China', *Water Science and Technology*, 84: 1257-69.

Zito, Phoebe, David C. Podgorski, Joshua Johnson, Huan Chen, Ryan P. Rodgers, François Guillemette, Anne M. Kellerman, Robert G. M. Spencer, and Matthew A. Tarr. 2019. 'Molecular-Level Composition and Acute Toxicity of Photosolubilized Petrogenic Carbon', *Environmental Science & Technology*, 53: 8235-43.

Appendix: Supporting Information

Offloading event data.

Offloading Event	Offloading Date	GS Tank Level Prior Offload (ft)	GS Tank Level After Offload (ft)	Volume of Ballast Offloaded (x10^6 L)
1	1/16/2022	16.0	33.1	23.5
2	2/5/2022	21.1	27.4	8.7
3	2/11/2022	21.8	36.8	20.6
4	3/18/2022	18.1	32.0	19.1
5	3/24/2022	24.0	34.8	14.8
6	10/19/2022	13.5	29.4	21.9
7	10/30/2022	9.3	26.2	23.2
8	11/3/2022	17.3	33.5	22.3
9	11/5/2022	27.7	41.7	19.2
10	11/26/2022	20.9	34.7	19.0
11	12/10/2022	21.7	32.4	14.8
12	12/28/2022	7.0	23.3	22.4

Table S1. ICP-QQQ operating conditions.

Parameter	He	NH_3
Scan Mode	MS/MS	
Plasma Mode	HMI-8	
RF Power (W)	1600	
Sampling Depth (mm)	10	
Nebulizer Gas (L/min)	0.7	
Nebulizer Pump (reps)	10	
S/C Temp ©	2	
Dilution Gas (L/min)	0.28	
Octapole Bias (V)	-20	-5
Octapole RF (V)	180	
Cell Entrance (V)	-50	
Cell Exit (V)	-70	-60
Deflect (V)	-2	5
Plate Bias (V)	-60	
Cell Gas (mL/min)	5	30%
KED (V)	5	-7

Table S2. ICP-QQQ specific analyte information. Limit of detection (LOD) calculated by 3σ/slope; limit of quantification (LOQ) calculated by 10 σ/slope.

Isotope	Gas Mode	Integration Time	ISTD	LOD (µg/L)	LOQ (µg/L)
107 Ag	He	0.3	72 Ge	0.273	0.909
27 Al	He	0.3	45 Sc	0.568	1.893
75 As	He	1	72 Ge	0.233	0.777
137 Ba	He	0.1	45 Sc	0.236	0.788
111 Cd	He	1	45 Sc	0.004	0.014
59 Co	He	0.3	72 Ge	0.004	0.014
52 Cr	NH_3	0.5	103 Rh	0.027	0.091
63 Cu	He	0.3	72 Ge	0.059	0.197
56 Fe	He	0.3	72 Ge	0.279	0.929
55 Mn	He	0.3	72 Ge	0.128	0.426
95 Mo	He	0.3	72 Ge	0.009	0.031
60 Ni	He	0.3	72 Ge	0.104	0.347
208 Pb	He	0.3	72 Ge	0.010	0.032
121 Sb	He	0.3	72 Ge	0.017	0.057
232 Th	He	0.1	72 Ge	0.003	0.009
238 U	He	0.1	72 Ge	0.001	0.003
51 V	NH_3	0.5	103 Rh	0.002	0.007
66 Zn	He	0.3	72 Ge	0.462	1.538

Table S3. HOPs characterization data. ($N_{GS,\ DAF,\ Effluent}$ = 12, N_{TP} = 7)

HOPs Characterization Metric		Tank Prior		Gravity Separation		Dissolved Air Flotation		Effluent	
		Avg.	SE	Avg.	SE	Avg.	SE	Avg.	SE
Quantity	BTEX (mg/L)	--	--	7.47	1.05	0.09	0.02	0.01	0.00
	NVDOC (mg/L)	2.71	0.32	2.92	0.15	3.07	0.41	2.31	0.31
Optical	C1 (%)	51.96	1.92	54.12	2.30	25.93	2.37	21.87	1.78
	C2 (%)	20.81	1.09	24.26	2.69	34.62	2.35	34.79	1.45
	C3 (%)	18.57	0.66	15.38	1.27	26.74	1.50	30.36	0.48
	C4 (%)	8.66	0.65	6.24	1.03	12.72	1.26	12.98	1.13
	HIX (RSU)	0.282	0.010	0.262	0.013	0.376	0.026	0.374	0.014
	$SUVA_{254}$ (L mg^{-1} cm^{-1})	0.013	0.001	0.009	0.001	0.010	0.002	0.008	0.001

Table S4. Metric correlations through the treatment process (Spearman's correlation coefficient (ρ) 95% confidence). (* indicates non-significant correlation)

HOPs Metric		Spearman's Correlation Coefficient (ρ)	p-value
Quantity	BTEX	-0.9170	< 0.0001
	NVDOC*	-0.192*	0.2175*
Optical	C1	-0.8045	< 0.0001
	C2	0.7127	< 0.0001
	C3	0.4537	< 0.0001
	C4	0.5441	0.0002
	HIX	0.6925	< 0.0001
	$SUVA_{254}$	-0.3454	0.0233

HMs Metric	Spearman's Correlation Coefficient (ρ)	p-value
Al	-0.8195	< 0.0001
As	-0.4554	0.0032
Ba	-0.3699	0.0188
Cr	-0.7730	< 0.0001
Fe	-0.8568	< 0.0001
Ni	-0.5214	0.0006
V	-0.5317	0.0004
THM	-0.8136	< 0.0001

Table S5. HM concentration levels (µg/L) ($N_{GS,Effluent}$ = 12, N_{TP} = 7, N_{DAF} = 9)

HM Metric	Tank Prior		Gravity Separation		Dissolved Air Flotation		Effluent	
	Avg.	SE	Avg.	SE	Avg.	SE	Avg.	SE
Ag	0.777	0.932	3.54	1.28	2.75	0.281	2.26	0.415
Al	13.1	0.0970	12.6	0.0956	3.70	0.0444	3.43	0.0248
As	2.46	0.0463	4.28	0.0164	2.30	0.0114	1.67	0.0117
Ba	82.9	1.29	72.5	3.69	65.5	7.30	60.5	10.1
Cd	0.0337	30.2	0.0177	25.7	0.0351	0.379	0.0343	0.300
Co	0.527	0.0793	0.205	0.0400	0.323	0.0630	0.408	0.105
Cr	0.249	2.02	0.189	3.93	0.0916	24.4	< 0.091	3.31
Cu	2.25	0.517	0.539	0.207	23.7	9.06	1.34	0.129
Fe	203	3.36	157	3.52	2.28	5.01	1.51	2.00
Mn	17.8	0.394	17.0	0.462	24.8	0.195	30.0	0.206
Mo	5.07	0.861	6.32	0.654	5.82	0.430	4.50	0.443
Ni	13.8	0.416	21.3	0.541	52.7	0.338	5.69	0.375
Pb	0.0184	0.0201	0.0571	0.00358	0.0473	0.0062	< 0.031	0.0120
Sb	0.184	0.0149	0.195	0.0196	0.201	0.0242	0.163	0.00821
Th	< 0.009	6.28	0.0383	6.57	< 0.009	4.84	< 0.009	4.15
U	0.428	0.00504	0.868	0.0108	0.733	0.0140	0.546	0.00401
V	0.368	0.000972	0.712	0.0159	0.198	0.00124	0.148	0.00130
Zn	30.1	0.139	31.44	0.150	31.4	0.0690	30.3	0.0387
THM	373	29.7	329	29.5	217	33.3	143	11.0